

# Experimental and numerical analysis of tribological effective surfaces for forming tools in Sheet-Bulk Metal Forming

Petra Kersting<sup>1</sup> · Daniel Gröbel<sup>2</sup> · Marion Merklein<sup>2</sup> · Peter Sieczkarek<sup>3</sup> · Sebastian Wernicke<sup>3</sup> · A. Erman Tekkaya<sup>3</sup> · Eugen Krebs<sup>1</sup> · Dennis Freiburg<sup>1</sup> · Dirk Biermann<sup>1</sup> · Tim Weikert<sup>4</sup> · Stephan Tremmel<sup>4</sup> · Dominic Stangier<sup>5</sup> · Wolfgang Tillmann<sup>5</sup> · Steffen Matthias<sup>6</sup> · Eduard Reithmeier<sup>6</sup> · Maria Löffler<sup>2</sup> · Florian Beyer<sup>7</sup> · Kai Willner<sup>7</sup>

Received: 3 September 2015 / Accepted: 7 December 2015 / Published online: 7 January 2016  
© German Academic Society for Production Engineering (WGP) 2016

**Abstract** Sheet-Bulk Metal Forming (SBMF) allows the manufacture of complex parts with integrated functional form elements, such as teeth and thickened areas. Therefore, bulk forming operations are applied to sheets with initial thicknesses of 2 or 3 mm. The design and functionality of the tools are as important as the process itself. Therefore, the working group “Tools” of the Transregional Collaborative Research Centre on Sheet-Bulk Metal Forming (CRC/TR73) focuses on the optimization of the technical tool design. By varying topographies or applying

tailored coatings, the friction behavior is changed to achieve a better form filling and to reduce process forces during the forming operations. In this paper, the potential of different tailored surfaces is validated by simulations and experimental studies. The tribological behavior of 14 surface microstructures is evaluated using a half-space model in order to select structures suitable for application. Those were characterized experimentally by ring-compression and pin-extrusion tests. The determined friction factors were used in a forming simulation to predict the form filling of small cavities in a flow forming operation. Furthermore, special attention is paid to the utilization of the anisotropic behavior of specific structures. The results were validated by an incremental gear forming process.

✉ Eugen Krebs  
krebs@isf.de

Petra Kersting  
petra.kersting@isf.de

<sup>1</sup> Institute of Machining Technology (ISF), TU Dortmund University, Baroper Str. 303, 44227 Dortmund, Germany

<sup>2</sup> Institute of Manufacturing Technology (LFT), Friedrich-Alexander-University Erlangen-Nürnberg, Egerlandstr. 11-13, 91058 Erlangen, Germany

<sup>3</sup> Institute of Forming Technology and Lightweight Construction (IUL), TU Dortmund University, Baroper Str. 303, 44227 Dortmund, Germany

<sup>4</sup> Chair of Engineering Design (KTmfk), Friedrich-Alexander-University Erlangen-Nürnberg, Martensstr. 9, 91058 Erlangen, Germany

<sup>5</sup> Institute of Materials Engineering (LWT), TU Dortmund University, Leonhard-Euler-Str. 2, 44227 Dortmund, Germany

<sup>6</sup> Institute of Measurement and Automatic Control (IMR), Leibniz University Hannover, Nienburger Str. 17, 30167 Hannover, Germany

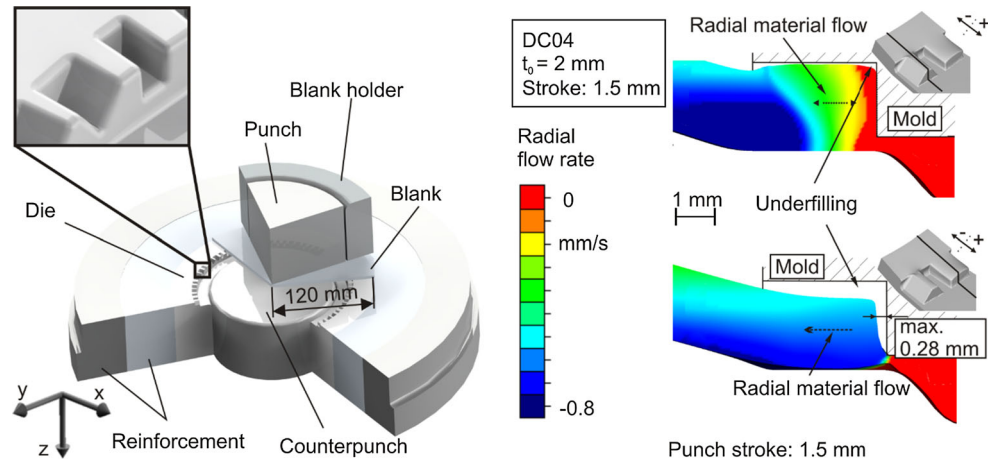
<sup>7</sup> Chair of Applied Mechanics (LTM), Friedrich-Alexander-University Erlangen-Nürnberg, Egerlandstr. 5, 91058 Erlangen, Germany

**Keywords** Sheet-Bulk Metal Forming · Tailored surfaces · Milling technologies · Coating technologies · Forming simulations · Tribology simulation

## 1 Challenges of Sheet-Bulk Metal Forming

Sheet-Bulk Metal Forming (SBMF) processes are mainly used to form local functional elements from a sheet plane with a dimension magnitude similar to the thickness of the sheet. This leads to a complex interaction between the forming zones with locally varying 2D and 3D stresses and strain states [1]. As a consequence, a major challenge of SBMF processes is the control of the material flow during the forming operation [1]. Due to the high strain gradient between the forming zone of the functional elements and the remaining blank area, a distinct material flow in the sheet plane can be observed, which subsequently results in an insufficient forming of the elements. One characteristic process is depicted in Fig. 1a. The process is categorized as

**Fig. 1** Process setup (a) and simulated underfilling of the elements after forming (b) [2]



a flow forming operation and aims to produce parts with circularly arranged, rectangular as well as triangular shaped elements out of a blank. Due to the high process forces for this class of processes, the die is reinforced and hardened (60 HRC).

Recent experimental and simulation-based investigations have analyzed the interaction of the material flow with respect to the shape and arrangement of different cavity geometries with a global friction factor of 0.12 [2]. Although the cavity geometry influences the material flow in the molds itself, a distinct underfilling could be observed in the triangular as well as in the rectangular cavity. Figure 1b visualizes this circumstance by means of the corresponding flow rate in radial direction for a cut through the molds.

One strategy to compensate this underfilling is to redirect the radial material flow into the molds by means of locally adapted friction conditions on the workpieces or tools. From a theoretical perspective, a favorable influence can be obtained if the friction factor is increased as much as possible in the area surrounding the cavities, while at the same time keeping the friction factor in the mold as low as possible [3]. The unfavorable material flow in the sheet plane is impeded, whereas the flow into the mold itself is facilitated. Current research showed that this strategy is effective if tailored surfaces are applied on the flow forming tool of Fig. 1 and the corresponding semi-finished blank. Thereby, an improvement of the mold filling of up to 12 % could be achieved [4].

Mold filling is also an important aspect in the incremental procedure, which is investigated as a flexible SBMF process. Previous studies showed that the incremental procedure requires a maximum chamfering of the workpiece to restrict the lateral material flow [5]. Limited by the chamfering system, the maximum tool size has to be of the same magnitude as the thickness of the sheet metal (Fig. 2a). Due to the high loads during the forming

process, an early deformation or failure of the small tools results in an insufficient process reliability (Fig. 2b). Hence, the reduction of process forces constitutes an important issue. Structured tool surfaces are one method to reduce the forces in the incremental gear forming process. Tailored surfaces, produced by micromilling for example, showed a process force reduction of about 20 % [6].

## 2 Surface modifications by tailored surfaces

Different surface modifications are investigated to optimize SBMF processes. In particular, the manufacturing of different surface microstructures and coating technologies are taken into consideration. The manufacturing of structures is realized by two milling processes. To structure large areas on the forming tools in a short time, a high-feed milling process was developed. High-feed milling is established for roughening operations and the milling of hard materials, but it can also be used to adapt surfaces by creating specific microstructures [7]. In Fig. 3, a selection of seven structures (HF1–HF7) is presented. The variation with regard to shape, size, and orientation of the feed marks is realized by a change of the cutting parameters and tool geometry.

The second class of surfaces (MS1–MS7) is produced by a micromilling process. Micromilling is suitable for machining geometrically defined surface structures onto smaller, more complex areas [6]. As visualized in the figure, the milled structures show round, oval, and lengthly shaped elements in different size, distance, and orientation. Both processes were performed after the hardening of the material and hence constitute a finishing hard milling operation [8].

In order to protect the surfaces and thus the forming tools from wear and to adapt the friction between tool and workpiece, tribological aspects can be optimized by means

**Fig. 2** Schematic illustration of the incremental gear forming process (a). Tool failure (b) [5]

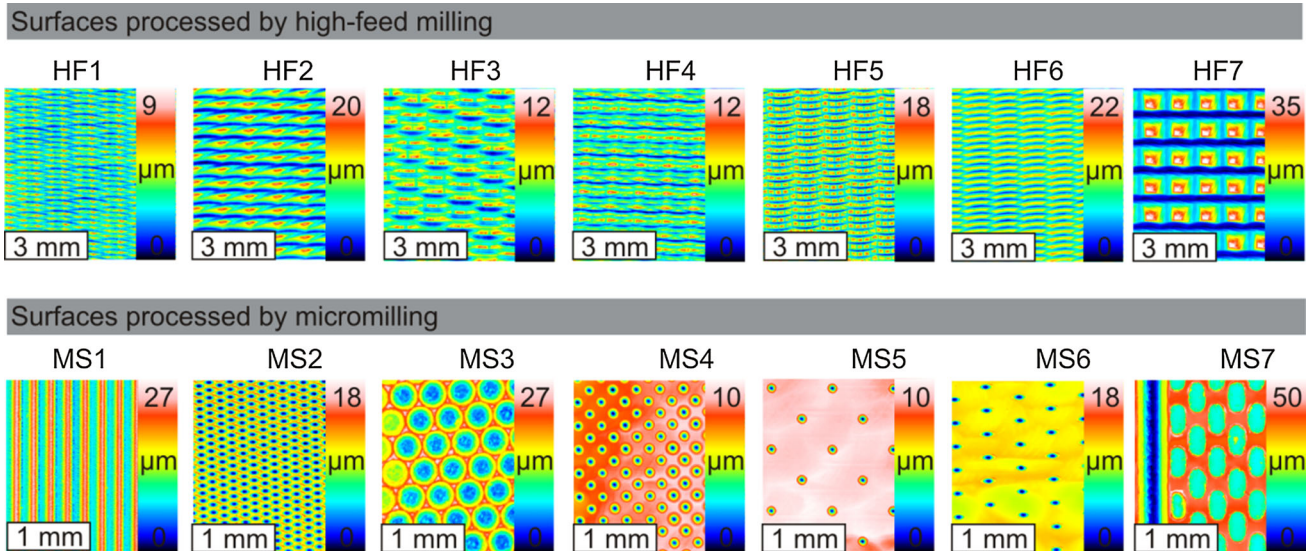
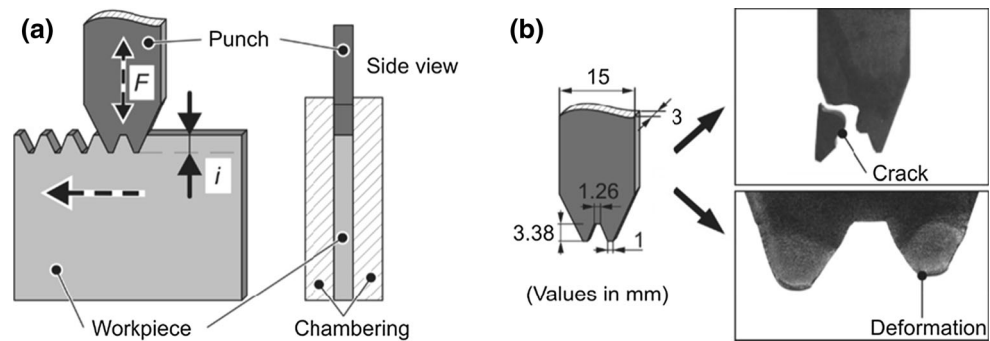


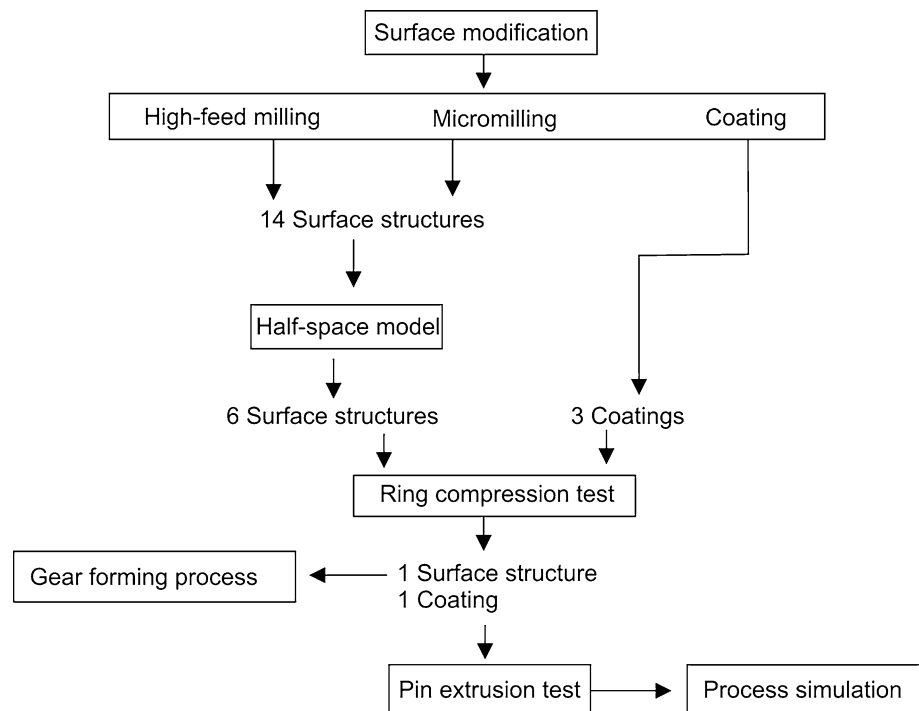
**Fig. 3** Overview of surface structures machined by high-feed milling (HF) and micromilling (MS)

of ceramic and diamond-like carbon (DLC) coatings. Within the class of DLC coatings, especially tungsten-modified amorphous carbon coatings (a-H:W) provide a high loading capacity. Moreover, the tribological properties can be adjusted by adapting the parameter values of the deposition process. The investigation of the tribological-mechanical behavior under high contact pressures in load-scanning tests [9] of the selected a-C:H:W variant revealed a constantly low friction and only little adhering of the steel to the coated surface. Since the adhesion of steel is assumed to be an initial damage mechanism of a C:H:W coating [10], this variant seems to be an adequate means to control the friction in SBMF processes. Besides a-C:H:W coatings, Cr-based ceramic coatings have shown to enhance the tribomechanical properties of highly stressed surfaces. Due to its wear resistance, especially CrAlN is suitable for the load spectrum of SBMF processes. To further improve the performance and to reduce the friction, carbon can be added to the ternary coating system, yielding CrAlCN coatings [11].

### 3 Procedure model

To examine the potential of tailored surfaces by different surface modifications, tribological investigations are required. High expenditure and a partially complex feasibility of some tribological tests can inhibit this realization for numerous structures and coatings. Hence, a new hierarchical approach combining individual works within the TR73 is utilized within this research. The procedure is shown in Fig. 4. To reduce the experimental characterization, the tribological behavior of the 14 surface microstructures was determined on the basis of a mechanical-rheological half-space model. Only six suitable structures were chosen for experimental tests. These surface structures, as well as the three coatings, were evaluated by a ring-compression test. Special attention was paid to the utilization of the anisotropic behavior of specific structures. In a next step, one coating and one surface structure were selected for an evaluation in the pin-extrusion test in order to determine the friction factors. The

Fig. 4 Procedure model



friction factors  $m$  were used in a simulation to predict the form filling of small cavities in a flow forming operation. Finally, the surface structure with the highest anisotropic friction behavior was applied onto a gear tooth tool and tested in a gear forming process.

#### 4 Numerical and experimental results

In the following section, the surface structures motivated in Sect. 2 are evaluated by means of experimental and simulative characterization methods. The selection of structures for the different tests and the sequence, in which the tests are described, follow the procedure model presented in Sect. 3 and depicted in Fig. 4.

##### 4.1 Advanced approach for the characterization of tailored surfaces using an elastic–plastic half-space model

The tribological analysis of microstructures in a simulation requires a characterization of the surface topography. Typical technical surfaces, as produced by finishing processes like grinding, polishing, or EDM can be described by the roughness profiles and two dimensional surface parameters. However, tailored surfaces are characterized by a deterministic roughness distribution, which demands a more sophisticated approach. One option is the mechanical-rheological model described in [12, 13], which is based

on three-dimensional surface parameters. The mechanical-rheological model is suitable for mixed lubrication and sections the surface as shown in Fig. 5a. The material ratio  $\alpha_{ma}$  describes the proportion of the solid area and is compliant with the real contact area denoted by  $\alpha_{cl}$ , which is the area that is in contact due to the surface asperities. The important value  $\alpha_{ma}$  is used to determine typical, three-dimensional surface parameters, namely the peak material volume  $V_{mp}$ , the core material volume  $V_{mc}$ , the core void volume  $V_{vc}$ , and the dale void volume  $V_{dv}$  which are explained in detail in [14]. In Fig. 5a, the closed void area is surrounded by a solid area, which enables it to transmit hydrostatic pressure between the contact partners. The share of the closed void area on the total area  $A_0$  is defined as  $\alpha_{cl}$ . Similarly, the ratio  $\alpha_{op}$  denotes the share of the open void area which is connected to the boundary of the loaded area. As the lubricant can be squeezed out in this section, this part of the area is not capable to build up a hydrostatic pressure. Figure 5b shows  $\alpha_{ma}$ ,  $\alpha_{cl}$ , and  $\alpha_{op}$  in dependency of the penetration depth for a typical example.

Technical surfaces initially get into contact with their surface peaks. As  $\alpha_{ma}$  is small in this case, the local contact pressure is large enough to plastically deform the surface asperities—even with a low nominal surface pressure  $p_0$ . The elastic–plastic contact impacts  $\alpha_{ma}$ , which is important for the friction, as tangential contact loads are only transferable in  $\alpha_{ma}$ . The interdependency between  $p_0$  and  $\alpha_{ma}$  cannot be described with surface parameters. Studying this interdependency is a highly complex task. Therefore, a

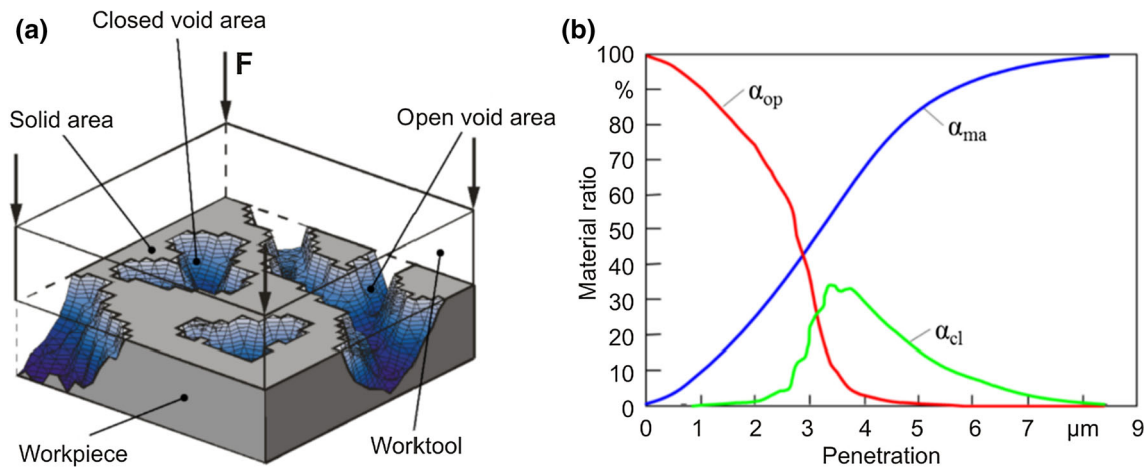


**Fig. 5** Distribution of a surface according to mechanical-rheological model [18] (a). Material ratio in dependency on the penetration (b)

numerical identification is performed. The accurate representation of the multi-scale character of the rough surface needs both a very fine resolution and a large area to be discretized. An elastic–plastic half-space model is chosen for the numerical identification, because it only requires a discretization of the contacting surfaces and, thus, has the advantage that the numerical effort is significantly reduced compared to standard FEM [15]. The half-space model was successfully calibrated for the contact simulation of a DC04 sheet material [16]. Furthermore, the mechanical-rheological model can be integrated [17], which makes it possible to determine  $\alpha_{ma}$ ,  $\alpha_{cl}$ , and  $\alpha_{op}$  in dependency on  $p_0$ . The half-space model in conjunction with the mechanical-rheological model is used to qualitatively assess different surface structures. The criterion is the ability to transfer friction stresses in dependency on  $p_0$ . However, the model is not able to quantitatively determine a friction coefficient. If this is required, an experimental determination is still necessary.

#### 4.2 Simulation of tribological behavior

The elastic–plastic half-space model with the implemented mechanical-rheological model was used to simulate the normal contact of the structured surfaces. The contact partner for the surfaces was an electric discharge texture (EDT) of a sheet metal with an average roughness of  $R_a = 1.010 \mu\text{m}$ . The EDT is a typical rough surface for SBMF. The contact load  $p_0$  ranged from 0 to 600 MPa in steps of 25 MPa. A square-shaped section of each surface, with a length of 2.56 mm and a discretization of 256 elements in each lateral direction, was used in the simulation. The structured surfaces were treated as solely elastic, whereas the sheet metal surface was considered to be elastic–plastic. Figure 6 shows the determined results for the 14 microstructures of Fig. 3 regarding the material ratio

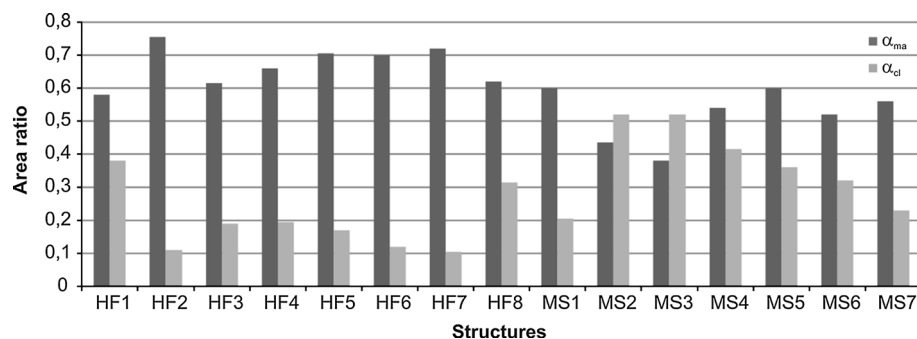
$\alpha_{ma}$  and the closed void area  $\alpha_{cl}$ . All 14 structures show a high variety of  $\alpha_{ma}$  and  $\alpha_{cl}$  values which can be used to adjust the friction behavior in forming processes. For further examination in experimental studies, three surfaces with different  $\alpha_{ma}$  and  $\alpha_{cl}$  values for each manufacturing technology were selected. From the high-feed milling process, structures HF1–HF3 were chosen. From the structures machined by micromilling, MS1–MS3 were selected for further investigations. HF1 and MS2 show the highest  $\alpha_{cl}$  values within the group. For these structures, a high potential of transmitting the hydrostatic pressure, resulting in a low friction coefficient, can be expected. HF2 and MS1 obtain the lowest  $\alpha_{cl}$  values. HF2 also presents the structure with the highest material ratio  $\alpha_{ma}$ . For these structures, high friction coefficients are expected. HF3 shows the same  $\alpha_{ma}$  value as HF1, but is positioned between HF1 and HF2 with regard to the closed void area. MS3 is selected due to its combination of high  $\alpha_{cl}$  and the smallest  $\alpha_{ma}$  values.

For more detailed information, results of the chosen structures HF1, HF2, HF3, MS1, MS2, and MS3 are depicted in Fig. 7, which shows  $\alpha_{ma}$ ,  $\alpha_{cl}$ , and  $\alpha_{op}$  in dependency on  $p_0$  for each surface.

#### 4.3 Tribological behavior of surface structures

In addition to the simulation by means of the half space model, an experimental evaluation of the friction characteristics for specific surfaces was performed. For a non-destructive measurement of the surface topographies, a confocal laserscanning microscope Keyence VK-X210 with a lateral resolution of 2 nm and a height resolution of 0.5 nm was used. For each surface topography, the measurements were stitched to an area of  $6000 \mu\text{m} \times 6000 \mu\text{m}$ . The roughness parameters and surface characteristics were calculated according to DIN EN ISO 4287

**Fig. 6** Characterization of 14 microstructures using a half-space model



and were analyzed using the software Nanofocus  $\mu$ soft analysis. Sections of the measurements ( $2000 \mu\text{m} \times 2000 \mu\text{m}$ ), roughness parameter values, and characteristics are presented in Fig. 7.

The experimental testing was conducted by using a ring-compression test (RCT) according to [19]. The experimental setup is shown in Fig. 8. The test was repeated five times for each surface topography and sheet metal (DC04 and DP600). To ensure stable forming grades, a distance ring of 1 mm was used. This means that all rings were compressed from 2 mm to 1 mm in thickness. The exact positioning of the ring is guaranteed by a respective unit. The oil volume was regulated by a fine scaled syringe. The rolling direction of the specimens was marked and oriented on the X-direction of all surface structures.

To determine the inner radii of the rings, a tactile coordinate measuring machine Zeiss ZMC 550 was used. The inner contour of the rings was traced by a cylindrical measurement sensor with a radius of 1 mm. Depending on the length of the contour, measurement points in a range of 200 and 250 points were recorded. The 2D profiles were evaluated using the software MATLAB. For this purpose, the parameter values of the inner circle radii as well as the ellipse parameters in X and Y-direction were calculated.

The friction behavior of the surface can be determined, depending on the radii of the ellipse in X- and Y-direction after the forming process. A smaller friction coefficient indicates a larger inner radius, while a higher friction results in smaller radii [20]. The results for the high-feed and micromilled surfaces are presented in Fig. 9.

For DP 600, the radii are larger for both directions, indicating a lower friction compared to DC04. These results can be explained by the microstructure of the materials. Besides the ferrite, the dual phase steel DP600 contains martensite, which leads to a higher hardness and therefore to lower friction values. These results confirm the investigation of Rajnesh et al. [21] showing that higher martensite contents lead to lower friction coefficients for surfaces in contact with hardened steel.

Additionally, all analyzed structures show differences with regard to the direction (X- vs. Y-direction). On the

one hand, an anisotropic material behavior is caused by the rolling direction of the sheets. On the other hand, the different surface structures illustrate a significant influence on the material flow. The isolated effect of the surface structures can be determined by comparing a polished surface (PO) to the selected surfaces with a high and low material flow behavior. Surfaces machined by a polishing process show a more isotropic friction behavior compared to conventional surface treatments. Figure 10 presents the difference of the radii in X- and Y-direction, which indicates the anisotropy of each structure. The structure-independent anisotropic material behavior is visible for both materials and is marked by a dotted line. For DC04, the anisotropy of the sheets is smaller compared to DP600, but the ratio between the different surface structures show the same tendency. Depending on the structure, isotropic or anisotropic friction, and thus a control of the material flow, can be achieved. Using the micromilling and high-feed milling process, it was possible to create surfaces which can provide an almost isotropic (HF3, MS2) and a strongly anisotropic material flow (HF2, MS1). Depending on the surface used, the friction can be adapted to create a directional material flow. On the one hand, it is possible to impede the material flow in specific areas. On the other hand, the material flow can be facilitated to obtain a better form filling of small cavities.

#### 4.4 Tribological behavior of coated surfaces

Ring-compression tests were also conducted to investigate the influence of a-C:H:W, CrAlN, and CrAlCN coatings on the friction behavior of DC04 and DP600 steel. The obtained inner radii of the rings for differently coated forming tools and for a polished, uncoated reference tool are presented in Fig. 11.

Except DC04 in combination with a CrAlN-coated forming tool, all investigated samples show a directional dependence of the friction behavior due to the anisotropy of the sheet metal workpiece. In rolling direction (X-direction), the friction is generally smaller when compared to the orthogonal orientation due to the elongation of the

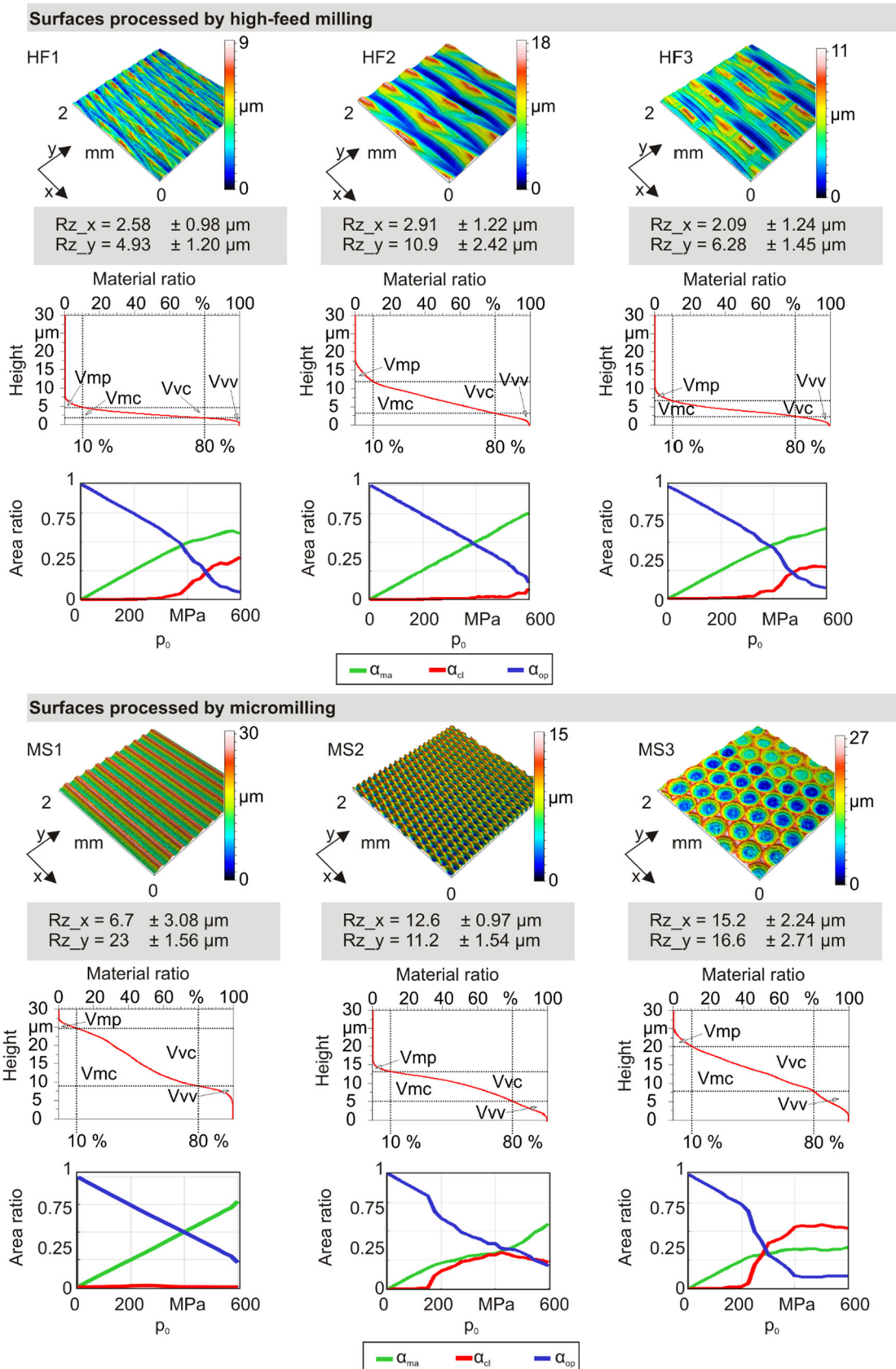


**Fig. 7** Confocal light pictures, Abbott-Firestone curve and area ratios determined by a hydrostatic elasto-plastic half space model

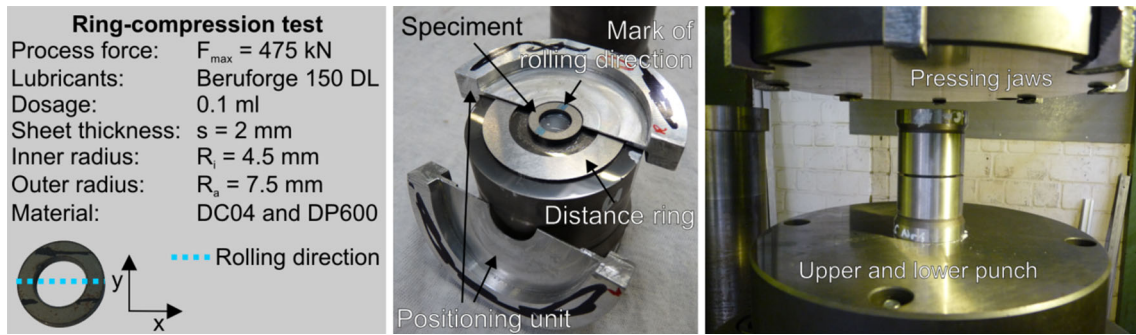


**Fig. 8** Experimental setup of the ring-compression test

**Fig. 9** Comparison of the structured surfaces based on measurements of the inner radii of the specimens made of DC04 and DP600 after the ring-compression test

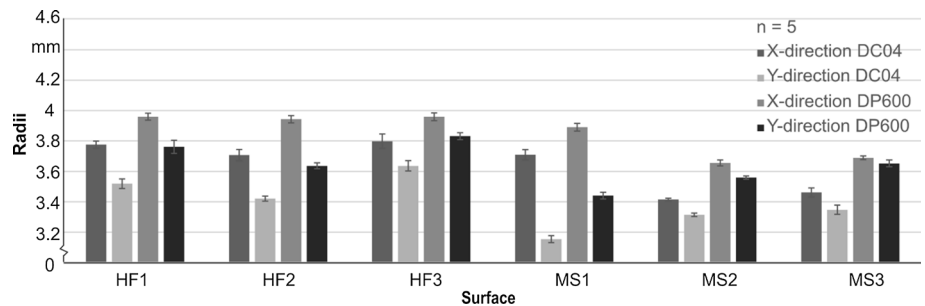


**Fig. 10** Radii difference between structured and polished surfaces for DC04 and DP600

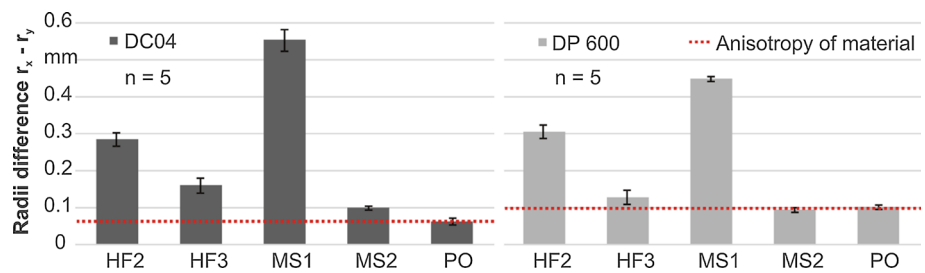
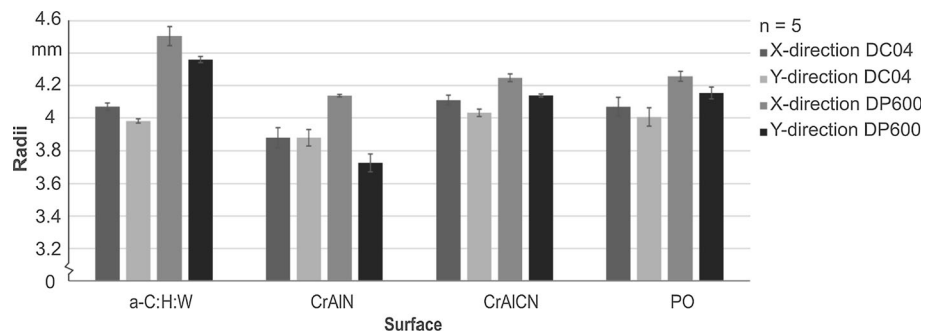


**Fig. 11** Results of ring-compression test for DC04 and DP600 with polished and coated forming tools



grains. Independent from the coating process, DP600 shows a lower friction compared to DC04 in the ring-compression test, confirming the previous results.

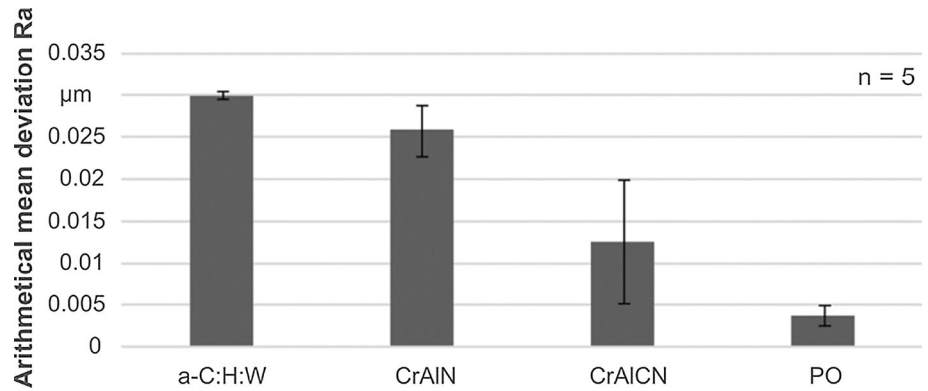
Beside the microstructure of the workpiece, the roughness of the coatings and its characteristics play an important role for friction conditions as well. Prior to the coating process, all punches were polished in the same way. After the coating process, different roughness values accrued.

The a-C:H:W- and CrAlN-coated punches show the highest roughness values (Fig. 12).

The incorporation of carbon into the nanocrystalline structure of (CrAl)N results in lower roughness values which lead to the formation of a friction reducing amorphous carbon phase [11]. Furthermore, it can be expected that tribochemical reactions of a-C:H:W coatings with extreme pressure (EP) additives of the forming oil, lead to



**Fig. 12** Surface roughness of forming tools



the formation of  $WS_2$  compounds, which act as an additional solid lubricant [22].

#### 4.5 Determination of friction factors using a pin-extrusion test

The results of the ring-compression test, shown in the previous sections, were used for a qualitative selection of suitable tool-sided surface modifications according to the requirements of SBMF [23]. Figure 13 shows the results of the RCT for the modification with the lowest friction. This condition is fulfilled by a polished surface covered by an a-C:H:W coating, and the highest friction, generated by the application of the structure MS1. To confirm these results and to determine the friction factors for the simulation of the SBMF process, these modifications are comprehensively analyzed within a more process-oriented friction test.

The pin-extrusion test combines an upsetting and a forward extrusion process, which are typical SBMF operations. A pin is formed by pressing the upper die onto the sheet Fig. 14a. This friction test was adapted to the requirements in SBMF and validated [23]. Based on the results of the numerical validation, the lower die includes a cavity with an undercut with a diameter of 1.5 mm and a shoulder radius of 1.0 mm. The higher the friction, the

more material flows into the cavity due to the undercut. This results in an increased height of the pin and indicates an increased friction factor. For the experimental investigation, specimens made of DC04 and DP600 with a diameter of 20.0 mm and a sheet thickness of 2.0 mm were used. To determine the friction factor  $m$ , the height of the specimen after a defined punch stroke of 1.0 mm is used. The specimen’s height is given by the remaining specimen height after the punch stroke, including the height of the pin Fig. 14b. Thus, the used height of the specimen for the determination of the friction conditions is always higher than 1.0 mm, even if the forming is frictionless.

As there are no means to obtain the friction factor directly from the height of the specimen, the principle of numerical identification was applied Fig. 14b. The corresponding FE model of the pin-extrusion test was implemented in simufact.forming 11.0.2. Several friction factors  $m$  between 0.02 and 0.2 were simulated and a calibration curve was determined. Figure 15 illustrates exemplarily the numerically determined calibration curve of DC04. The curve is used to determine the friction factors of different tribological systems from the measured specimen heights. This approach is exemplarily shown in Fig. 15 for DC04 using the lubricant Beruforge 150DL.

To implement the pin-extrusion test, a deep drawing press Lasco 100SO with a traverse speed of 1.00 mm/s was

**Fig. 13** Results of the ring-compression test

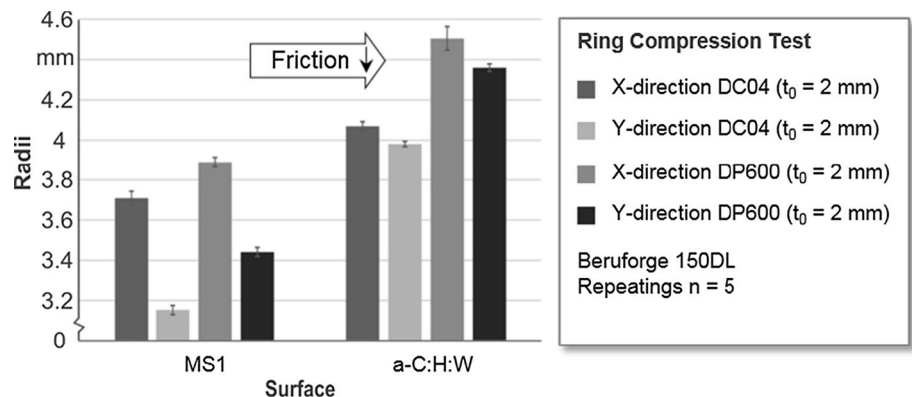


**Fig. 14** Pin-extrusion test (a) and measured specimen height after testing (b)

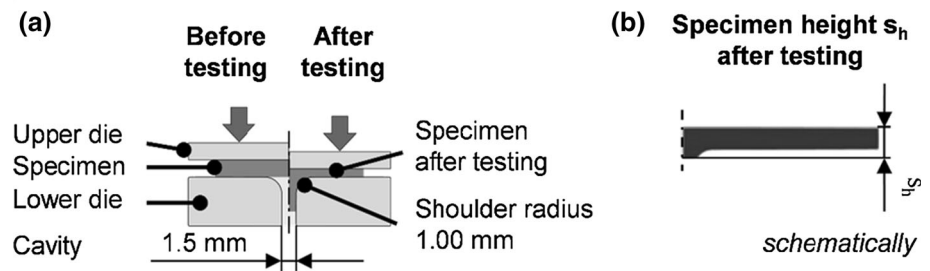


**Fig. 15** Principle of numerical identification using the numerically determined calibration curve of DC04

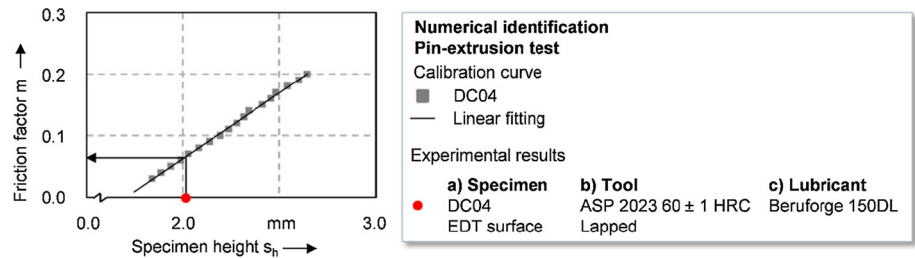
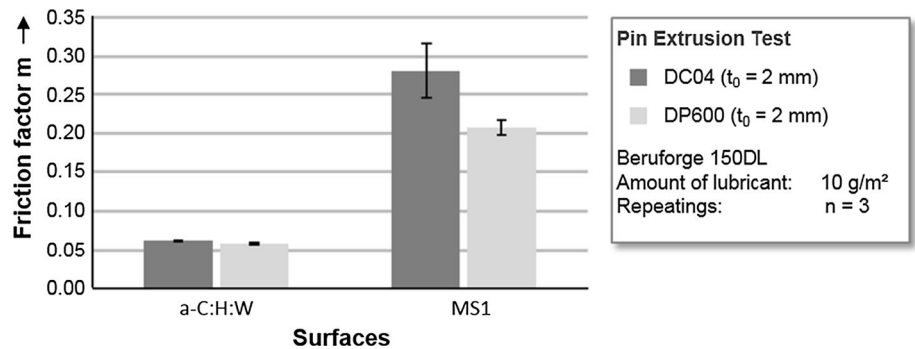


**Fig. 16** Results of the pin-extrusion test



used. Three workpieces were tested to increase the statistical reliability. Figure 16 illustrates the results of the pin-extrusion test for both surface modifications and materials. The results confirm that the coated surface leads to a lower friction than the microstructure. The friction factor of the a-C:H:W surface on DC04 amounts to  $0.06 \pm 0.01$ . For DP600, a friction factor of  $m = 0.058 \pm 0.01$  was determined. In comparison, the friction factor of structure MS1 has a value of  $0.28 \pm 0.03$  for DC04. The friction factor of DP600 amounts to  $0.21 \pm 0.01$ . The determined friction factors were used for a process-oriented numerical investigation of two SBMF processes which is described in the following section.

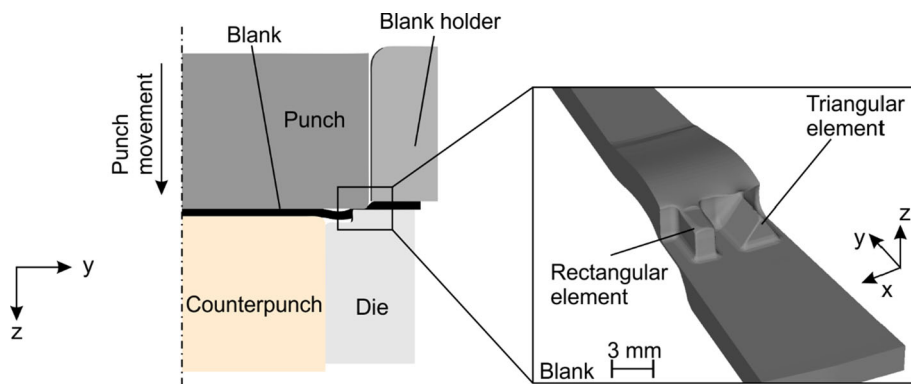
## 5 Process optimization by means of tailored surfaces

As described in chapter 1, the friction in the area surrounding the cavities should be as high as possible while the friction in the cavities themselves should be as low as

possible in order to facilitate the formation of functional elements. Based on this theory, the a-C:H:W coating and the structure MS1 were used to investigate the possibility to improve the flow forming process (Fig. 1) and the incremental flow forming process (Fig. 2) since the surface treatments possess the highest and the lowest friction factor, respectively.

Regarding the flow forming process, the investigation was conducted by means of the simulation model displayed in Fig. 17. The model resembles the process described in chapter 1 and has been validated by a geometrical comparison between the resulting and simulated workpiece in [2]. As it is the case in the real process, a blank of 120 mm in diameter is centrally placed on a die that entails corresponding cavities. Subsequently, the blank is clamped between the punch and the counterpunch. Additionally, a blank holder is used to impede a bulging of the blank in the rim area. In order to conduct the operation, the punch is moved in z-direction which results in the formation of the functional elements displayed in Fig. 17 by flow forming. For the simulation, a v. Mises material model for DC04 is

**Fig. 17** Cut display of the simulation model and resulting geometry of the functional elements



utilized. The corresponding hardening curve was ensured by layer compression tests and was extended by means of a Hockett-Sherby extrapolation. In order to achieve a sufficient modeling of geometrical aspects, a general mesh edge length of 0.4 mm is used and additionally refined in the elemental area to an edge length of 0.05 mm. Since numerical calculation time is challenging, the model size is reduced to a 10° cut, which exploits the given process symmetry and effectively lowers numerical demands. To calculate the friction behavior in the process simulation, a shear model according to Tresca is utilized.

In order to conduct the simulated experiments, MS1 was applied on the punch, the counterpunch, the blank holder, and the die. Only a small circular area above the cavities was omitted and the a-C:H:W coating was applied. It was expected that the material flow in the sheet plane will be reduced by the high friction in the structured area. At the same time, it was assumed that the low friction factor of the a-C:H:W coatings would facilitate a material flow into the molds and therefore increase the mold filling. Figure 18 visualizes the corresponding tailored surfaces on the tool.

The values derived in the previous chapter were used as friction factors. In detail, friction factors of 0.062 (DC04) and 0.058 (DP600) were applied to resemble the a-C:H:W coated surfaces. In the same manner, values of 0.282 (DC04) and 0.207 (DP600) were used for the corresponding contact areas between the tool and blank, entailing the MS1 structure. Two simulation runs were conducted, one with DC04 and one with DP600, while all other process parameters remained constant. Subsequently, the results were compared to similar simulations that use a global friction factor of 0.12. For all simulations, blanks of 2 mm, a blank holder force of 360 kN, and an counter punch force of 400 kN were used. The punch stroke was equal for all simulations and amounts to 1.7 mm. For comparison, the mold filling, defined as the amount of material volume located in the mold at the desired stroke in relation to the absolute mold volume, was chosen. The results showed that the mold filling could be increased by 6.04 % for the rectangular element and by 0.19 % for the triangular element for DC04. Similar results were obtained for DP600: mold filling could be improved by 4.15 % for the rectangle and by 0.19 % for the triangle. The

**Fig. 18** Model, process parameters, and friction factors used for simulation

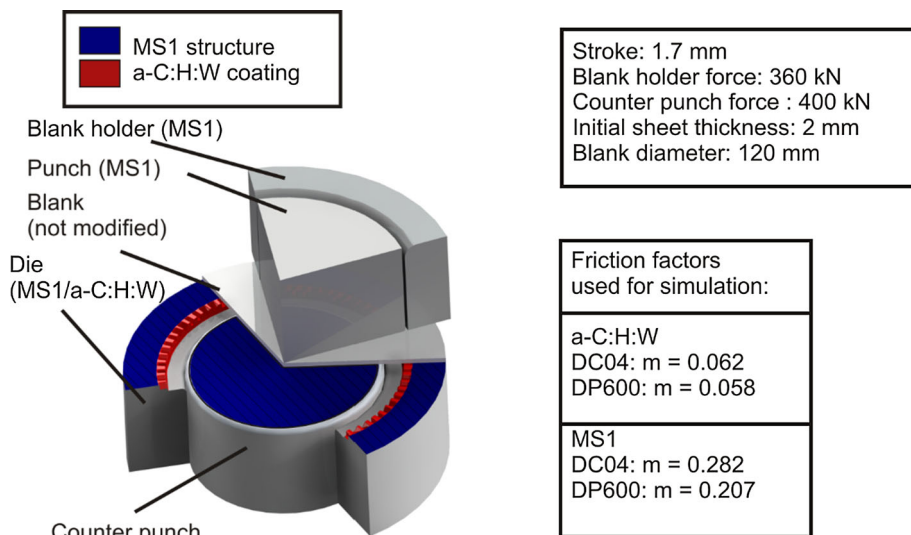


**Fig. 19** Resulting mold filling for the friction modified process and a reference model with a global friction factor of 0.12

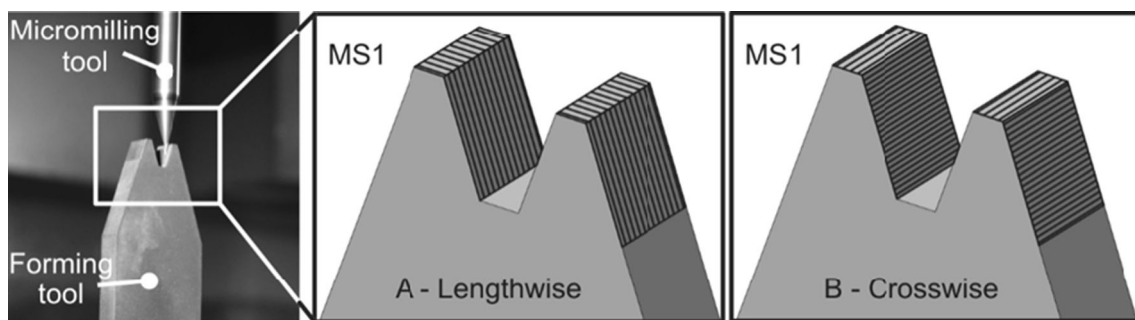
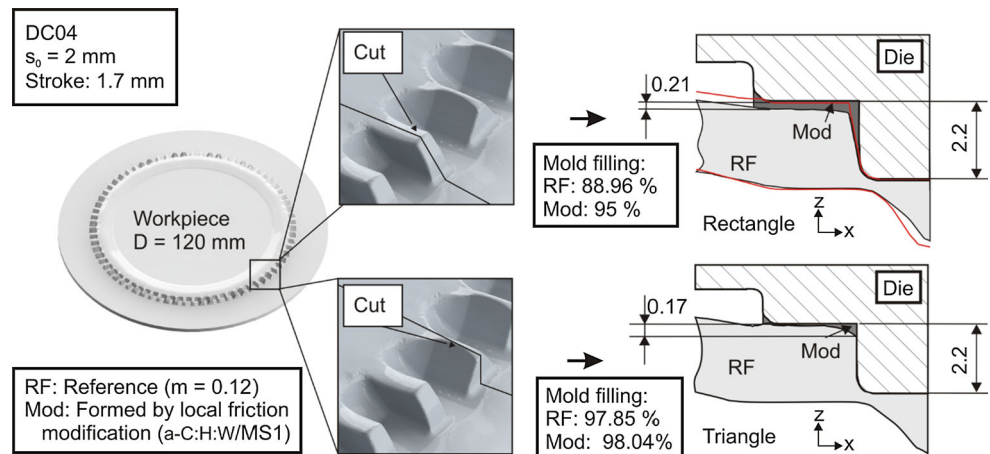


**Fig. 20** Structuring process of a forming tool using a micromilling process and schematic illustration of the microstructures on active surfaces, lengthwise and crosswise

differences between the rectangular and triangular elements can be explained by the fact that the mold filling of the latter is already much higher (approx. 95–90 %) in the reference simulation. This was expected due to the dependency of the mold the filling on the shape of the cavities, which was demonstrated in [2]. Since strain hardening increases with convergence to the maximum mold volume, a further improvement is more difficult to obtain. The exemplary cut, displayed in Fig. 19, confirms these findings, as the change in mold filling is mirrored by the increased element height in case of the modified simulation, using the evaluated friction factors  $m$  for both element types. At this point, it can be summarized that the use of a local friction modification is effective to improve the form filling for both DC04 and DP600 in case of the investigated forward flow forming process.

For the incremental gear forming process presented in chapter 1, two differently structured tools were used. The MS 1 structure was applied lengthwise (A) and crosswise (B) on the active surfaces of the geometrically identical tools (high-speed steel ASP2023, 63 HRC) by means of a micromilling process (Fig. 20). Determining the influence of the anisotropic behavior of the chosen structure on the prevailing material flow and on the forming forces was the

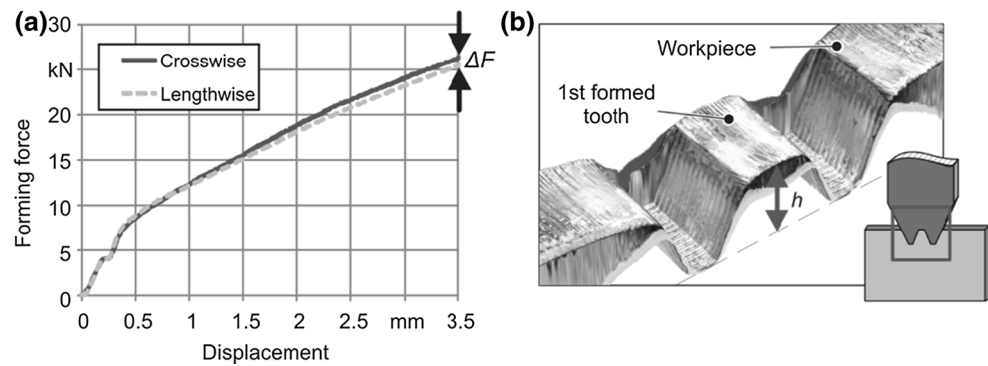
main objective. The experiments were conducted using a workpiece made of DC04 with a thickness of 3 mm. The indentation depth of the tool was 3.5 mm.

The experimental force–displacement curves (Fig. 21a) verify the anisotropic behavior of the MS1 structure also during the incremental gear forming process. The tools with the lengthwise structure, proved to have a lower friction coefficient (Fig. 9) and require a 3.5 % lower forming force than the crosswise structured tools. The measured mold filling of the shaped tooth geometry, simplified as the height  $h$ , shows a similar trend. Here, a 4 % higher mold filling could be achieved with the lengthwise structured tool (Fig. 21b). The results prove that microstructured surfaces are not only favorable in terms of forming forces, but also present an efficient means for the material flow adjustment. Based on the results in Fig. 9, this effect can be attributed to the reduced friction.

## 6 Summary and outlook

To ensure the product quality of Sheet-Bulk Metal Formed components, the tool design and characterization are the most important influencing factors. Therefore, the working

**Fig. 21** Force-displacement curves of the structured tools (a). Mold filling of the shaped tooth geometry (b)



group “Tools”, which is embedded in the Transregional Collaborative Research Center TR73, determines specific tool-sided optimization potentials. Within this paper, surface tailoring methods, coating processes, and experimental forming tests were performed. 14 different surface structures were machined utilizing high-feed and micromilling processes. It was possible to obtain specific surface structures with tailored characteristics. With a simulation of a half-space model, six surfaces resulting in a low and high pressure build-up were evaluated and selected for forming tests. Additionally, three different coating techniques were considered. Subsequently, the surface structures and both coating technologies, were evaluated in a ring-compression test to determine the friction behavior. In general, the results show lower friction values for DP600, which could be assigned to the higher hardness of the dual phase material. Structured surfaces show a major influence on the friction condition and allow the control of an anisotropic material flow by selecting specific structures. This notion was validated in an incremental gear tooth forming process. By depositing coatings to the surface, the roughness values were increased. The a-C:H:W coating, however, showed the best friction behavior among all modified surfaces. In addition to the ring-compression test, the friction factor was determined by a pin-extrusion test for selected surfaces with the highest and lowest friction values. Based on the evaluated factors, the advantages of tailored surfaces were presented in a validated FEM-based study. The form filling of small cavities could be increased up to 6.04 %. The presented results show the high potential of different surface techniques to optimize forming tools in SBMF processes.

**Acknowledgments** This work was supported by the German Research Foundation (DFG) within the scope of the Transregional Collaborative Research Centre on Sheet-Bulk Metal Forming (CRC/TR73, Workgroup “Tools”, Subprojects A2, A4, B2, B3, B4, B5, B6, and C1).

## References

- Merklein M, Allwood JM, Behrens B-A, Brosius A, Hagenah H, Kuzman K, Mori K, Tekkaya E, Weckenmann A (2012) Bulk forming of sheet metal. *CIRP Ann* 61(2):725–745
- Gröbel D, Koch J, Vierzigmann U, Engel U, Merklein M (2014) Investigations and approaches on material flow of non-uniform arranged cavities in sheet bulk metal forming processes. *Procedia Eng* 81:401–406
- Löffler M, Gröbel D, Engel U, Andreas K, Merklein M (2015) Analysis of effectiveness of locally adapted tribological conditions for improving product quality in Sheet-Bulk Metal Forming. *Appl Mech Mater* 794:81–88
- Hetzner H, Koch J, Tremmel S, Wartack S, Merklein M (2011) Improved Sheet Bulk Metal Forming Processes by Local Adjustment of Tribological Properties. *J. Manufacturing Science and Engineering* 133(6):61011-1-11
- Sieczkarek P, Kwiatkowski L, Tekkaya AE, Krebs E, Kersting P, Tillmann W, Herper J (2013) Innovative tools to improve incremental bulk forming processes. *Key Eng Mater* 554–557:1490–1497
- Sieczkarek P, Kwiatkowski L, Tekkaya AE et al (2012) Improved tool surfaces for incremental bulk forming processes of sheet metals. *Key Eng Mater* 504–506:975–980
- Freiburg D, Biermann D, Hense R, Stangier D, Tillmann W (2015) Influence of surface modifications on friction, using high-feed milling and wear resistant PVD-coating for sheet-metal forming tools. *Key Eng Mater* 639:275–282
- Suresh R, Basavarajappa S, Gaitonde VN, Samuel G, Davim JP (2013) State-of-the-art research in machinability of hardened steels. *Proc Inst Mech Eng Part B J Eng Manuf* 227(2):191–209
- Hogmark S, Jacobsen S, Wänstrand O (1999) A new universal test for tribological evaluation. In: *Proceedings of the 21st IRG-OECD Meeting*, Amsterdam, Netherlands
- Hetzner H, Schaufler J, Tremmel S, Durst K, Wartzack S (2012) Failure mechanisms of a tungsten-modified hydrogenated amorphous carbon coating in load-scanning tests. *Surf Coat Technol* 212:46–54
- Ahn S-K, Kwon S-H, Kim K-H (2011) Effect of carbon on microstructure of CrAlC<sub>x</sub>N<sub>1-x</sub> coatings by hybrid coating system. *Trans Nonferrous Met Soc China* 21:78–82
- Sobis T, Engel U, Geiger M (1994) A theoretical study of wear simulation in metal forming processes. *J Mater Process Technol* 34:233–240
- Pfistorf M, Engel U, Geiger M (1998) 3D-surface parameters and their application on deterministic textured metal sheets. *Int J Mach Tools Manuf* 38:607–614
- Leach R (2013) *Characterisation of areal surface texture*. Springer, Berlin
- Kalker JJ (1990) *Three-dimensional elastic bodies in rolling contact*, Vol 2. Springer, Netherlands
- Hauer F, Willner K (2013) Development of a Friction law respecting plastic surface smoothing. *Key Eng Mater* 554:1471–1477
- Hauer F (2014) Die elasto-plastische Einglättung rauer Oberflächen und ihr Einfluss auf die Reibung in der Umformtechnik.

- Erlangen, Germany, Friedrich-Alexander-University Erlangen-Nürnberg, Diss. (Schriftenreihe Technische Mechanik, ISSN 2190-023X)
18. Engel U, Neudecker T, Popp U (2000) 3D-Oberflächenanalyse - Methoden, Kenngrößen, Anwendungen. *Materialwiss Werkstofftech* 31:747–753
  19. Hense R, Kersting P, Vierzigmann U, Löffler M, Biermann D, Merklein M, Wels C (2014) High-feed milling of tailored surfaces for sheet-bulk metal forming tools. *Prod Eng Res Devel.* doi:[10.1007/s11740-014-0597-0](https://doi.org/10.1007/s11740-014-0597-0)
  20. Male AT, Cockcroft MG (1964) A method for the determination of the coefficient of friction of metals under condition of bulk plastic deformation. *J Inst Metal* 93:38–46
  21. Rajnesh T, Nath SK, Ray S (2002) Effect of martensite content on friction and oxidative wear behavior of 0.42 Pct carbon dual-phase steel. *Metall Mater Trans A* 33(11):3479–3488
  22. Hetzner H, Zhao R, Tremmel S, Wartzack S (2013) Tribological adjustment of tungsten-modified hydrogenated amorphous carbon coatings by adaption of the deposition parameters. In: Bouzakis MK-D, Bobzin K, Denkena B, Merklein M (eds) 10th international conference THE “A” Coatings. Shaker, Aachen, pp 39–49
  23. Vierzigmann U, Merklein M, Engel U (2010) tailored surfaces in sheet-bulk metal forming. In: Felder E, Montmitonnet P (ed) Proceedings of 4th international conference on tribology in manufacturing processes (ICTMP), Transvalor-Presses des MINES, pp 541–550